



ELSEVIER

Lithos 61 (2002) 271–282

LITHOS

www.elsevier.com/locate/lithos

# Pressure effect on Ti- or P-rich accessory mineral saturation in evolved granitic melts with differing $K_2O/Na_2O$ ratios

Trevor H. Green\*, John Adam

*GEMOC, Department of Earth and Planetary Sciences, National Key Centre, Macquarie University, Sydney, NSW 2109, Australia*

Received 29 November 2000; accepted 18 December 2001

## Abstract

The solubility of Ti- and P-rich accessory minerals has been examined as a function of pressure and  $K_2O/Na_2O$  ratio in two series of highly evolved silicate systems. These systems correspond to (a) alkaline, varying from alkaline to peralkaline with increasing  $K_2O/Na_2O$  ratio; and (b) strongly metaluminous (essentially trondhjemitic at the lowest  $K_2O/Na_2O$  ratio) and remaining metaluminous with increasing  $K_2O/Na_2O$  ratio (to 3). The experiments were conducted at a fixed temperature of 1000 °C, with water contents varying from 5 wt.% at low pressure (0.5 GPa), increasing through 5–10 wt.% at 1.5–2.5 GPa to 10 wt.% at 3.5 GPa. Pressure was extended outside the normal crustal range, so that the results may also be applied to derivation of hydrous silicic melts from subducted oceanic crust. For the alkaline composition series, the  $TiO_2$  content of the melt at Ti-rich mineral saturation decreases with increasing pressure but is unchanged with increasing K content (at fixed pressure). The  $P_2O_5$  content of the alkaline melts at apatite saturation increases with increased pressure at 3.5 GPa only, but decreases with increasing K content (and peralkalinity). For the metaluminous composition series (termed as “trondhjemitite-based series” (T series)), the  $TiO_2$  content of the melt at Ti-rich mineral saturation decreases with increasing pressure and with increasing K content (at fixed pressure). The  $P_2O_5$  content of the T series melts at apatite saturation is unchanged with increasing pressure, but decreases with increasing K content. The contrasting results for P and Ti saturation levels, as a function of pressure in both compositions, point to contrasting behaviour of Ti and P in the structure of evolved silicate melts. Ti content at Ti-rich mineral saturation is lower in the alkaline compared with the T series at 0.5 GPa, but is similar at higher pressures, whereas P content at apatite saturation is lower in the T series at all pressures studied. The results have application to A-type granite suites that are alkaline to peralkaline, and to I-type metaluminous suites that frequently exhibit differing  $K_2O/Na_2O$  ratios from one suite to another. © 2002 Elsevier Science B.V. All rights reserved.

*Keywords:* Granites; Accessory minerals; Apatite; Rutile; Silicate liquid structure; Fractionation

## 1. Introduction

The importance of trace element-enriched accessory minerals in governing the trace element content of magmas, either as minerals crystallizing from

fractionating magmas or as residual minerals in a source region undergoing partial melting, is well recognized (Green, 1981; Miller and Mittlefehdt, 1982; Gromet and Silver, 1983; Watson and Harrison, 1984; Sawka, 1988; Watt and Harley, 1993; Bea, 1996). P-rich (typically apatite) and Ti-rich (typically titanite or rutile) minerals are among the most ubiquitous of these accessory minerals in common magmas. In recognition of this, there have been many

\* Corresponding author. Fax: +61-2-9850-6904.

E-mail address: trevor.green@mq.edu.au (T.H. Green).

experimental studies directed at placing constraints on the potential role of apatite, titanite and rutile in magma genesis and evolution by establishing their solubility in common magmas as a function of magma composition, temperature and pressure (e.g. Watson, 1979; Green and Watson, 1982; Green and Pearson, 1986; Ryerson and Watson, 1987; Watson and Capobianco, 1981). These studies have determined “first order” controls of these variables, but magmas, as they evolve, can show more subtle yet nevertheless potentially significant “second order” compositional variations, such as differing  $K_2O/Na_2O$  and development of peralkaline or peraluminous character.

These second order compositional aspects are particularly relevant to granitic suites, where I-type magmas often exhibit different  $K_2O/Na_2O$  ratios, accentuated in the evolved members of the suites

(e.g. Bryant et al., 1997; Champion and Chappell, 1992; Chappell, 1999). In addition, granitic suites may show peraluminous or peralkaline character (e.g. Chappell, 1999; King et al., 1997). In order to evaluate the effect of these compositional parameters on apatite and Ti-rich phase solubility at depth of generation and subsequent shallower levels as the magmas rise towards the surface, it is necessary to carry out experiments on such compositions at high pressure. This has been the focus of the current study, where two composition series have been studied over a range of pressure, covering the crust and uppermost mantle.

The two composition series consisted of a metaluminous “trondhjemite-based series” (T series) and an “alkaline series”, both with variable K/Na, from 0.26 to 3.0 and from 0.6 to 1.7, respectively. These

Table 1  
Starting compositions (all normalized to 100%)

	Ti-series				P-series		
	DG	DG*Ti	DGTi	DGTiK	DG*P	DGP	DGPK
SiO <sub>2</sub>	61.88	61.30	59.68	58.21	62.24	60.49	58.63
TiO <sub>2</sub>	0.38	3.01	2.77	2.76	0.44	0.39	0.39
Al <sub>2</sub> O <sub>3</sub>	16.41	17.09	16.75	15.98	17.36	16.63	16.52
FeO	2.16	2.31	2.08	2.11	2.40	2.27	2.15
MgO	3.95	4.61	4.41	4.26	4.68	4.46	4.29
CaO	1.51	1.54	1.41	1.37	1.58	1.46	1.42
Na <sub>2</sub> O	6.26	6.27	5.88	5.69	6.47	6.00	5.91
K <sub>2</sub> O	7.46	3.81	6.99	9.56	4.01	7.10	9.56
P <sub>2</sub> O <sub>5</sub>					0.81	1.19	1.12
ASI	0.78	0.99	0.85	0.72	1.09	0.95 <sup>a</sup>	0.82 <sup>a</sup>
ALK	1.12	0.85	1.03	1.23	0.86	1.06	1.22
	TRN	TRNTi	TRNTiK	TRNTiKK	TRNP	TRNPK	TRNPKK
SiO <sub>2</sub>	65.32	67.21	65.50	64.59	65.30	64.46	64.41
TiO <sub>2</sub>	0.36	1.31	2.70	2.65	0.29	0.24	0.19
Al <sub>2</sub> O <sub>3</sub>	18.32	16.79	16.72	17.00	16.55	16.71	17.15
FeO	3.38	3.01	2.30	1.55	2.90	2.12	1.50
MgO	1.28	1.09	0.81	0.53	1.09	0.82	0.58
CaO	4.71	4.08	3.01	2.03	5.99	5.06	3.89
Na <sub>2</sub> O	5.28	5.08	3.97	2.86	4.99	4.00	2.73
K <sub>2</sub> O	1.35	1.42	4.97	8.78	1.39	5.02	8.19
P <sub>2</sub> O <sub>5</sub>					1.49	1.56	1.34
ASI	0.98	0.97	0.96	0.95	0.97	0.95	0.99
ALK	0.55	0.59	0.71	0.84	0.59	0.72	0.78

DG denotes the alkaline composition starting point, DG\* denotes the  $K_2O$  “reduced” compositions, Ti or P denotes the Ti or P added series and K denotes the  $K_2O$  “added” compositions, for the alkaline series. TRN denotes the trondhjemite starting point, Ti or P refers to the Ti or P added series and K or KK denotes the  $K_2O$  “added” compositions, for the metaluminous T series. ASI refers to the alumina saturation index (mol. prop.  $Al_2O_3/[CaO+Na_2O+K_2O]$ ) with peraluminous compositions having  $ASI>1$ . ALK refers to the alkalinity (mol. prop.  $[Na_2O+K_2O]/Al_2O_3$ ) with peralkaline compositions having  $ALK>1$ .

<sup>a</sup> Slight excess of  $P_2O_5$  over CaO (for apatite, 0.001–0.002 mol. prop.).

compare with  $K_2O/Na_2O$  of 0.4–1.7 in I-type and 1.1–1.8 in A-type granitic suites from eastern Australia (Bryant et al., 1997; Champion and Chappell, 1992; Chappell, 1999; King et al., 1997). The two composition series chosen also have relevance to subcrustal processes, justifying extending experimental pressures to those found in the upper mantle. Thus, the T series links in with possible melts (trondhjemitic) from low-degree hydrous melting of the subducted oceanic crust (e.g. Green, 1982), whereas the alkaline series is relevant to alkaline silica-undersaturated melts, recognized as possible metasomatic agents in the upper mantle (Draper and Green, 1997). No attempt has been made to evaluate compo-

sitional effects on accessory phase solubility for strongly peraluminous, S-type granitic series, as these have been established in some detail for apatite (Wolf and London, 1994; Mysen, 1998; Sha, 1998).

## 2. Experimental and analytical

### 2.1. Starting compositions

The T series were based on an average trondhjemite (Drummond and Defant, 1990) to which  $K_2O$  (in orthoclase component proportions) was added in two steps, and in two separate groupings,  $TiO_2$  and  $P_2O_5$

Table 2  
Analyses of glasses from the Ti-rich mineral saturated alkaline (DG) series

Composition	DG*Ti	DGTi	DGTiK	DG*Ti	DGTi
Run number	1851	1900	1900	1854	1854
Pressure (GPa)	0.5	0.5	0.5	1.5	1.5
Water (wt.%)	5	5	5	5	5
	<i>n</i> = 8 (S.D.)	<i>n</i> = 4 (S.D.)	<i>n</i> = 7 (S.D.)	<i>n</i> = 5 (S.D.)	<i>n</i> = 5 (S.D.)
SiO <sub>2</sub>	59.65 (0.12)	59.99 (0.28)	57.67 (0.39)	64.11 (0.29)	62.87 (0.29)
TiO <sub>2</sub>	2.25 (0.08)	2.25 (0.06)	2.32 (0.12)	0.91 (0.02)	1.16 (0.06)
Al <sub>2</sub> O <sub>3</sub>	16.86 (0.06)	16.15 (0.10)	15.80 (0.06)	18.49 (0.10)	17.21 (0.05)
FeO	1.77 (0.09)	1.63 (0.02)	1.65 (0.04)	0.85 (0.05)	0.78 (0.02)
MgO	2.31 (0.04)	1.79 (0.06)	1.84 (0.06)	0.96 (0.01)	0.76 (0.11)
CaO	1.52 (0.04)	1.48 (0.03)	1.42 (0.03)	1.28 (0.06)	0.76 (0.04)
Na <sub>2</sub> O	5.97 (0.08)	5.66 (0.08)	5.81 (0.07)	5.0 <sup>a</sup>	5.5 <sup>a</sup>
K <sub>2</sub> O	3.76 (0.06)	6.00 (0.06)	8.68 (0.06)	3.41 (0.04)	6.16 (0.06)
Total	94.09 (0.21)	94.99 (0.30)	95.24 (0.40)	95.01 (0.25)	95.20 (0.26)
Composition	DGTiK	DG*Ti	DGTi	DGTiK	
Run number	1854	1852	1852	1852	
Pressure (GPa)	1.5	2.5	2.5	2.5	
Water (wt.%)	5	10	10	10	
	<i>n</i> = 5 (S.D.)	<i>n</i> = 4 (S.D.)	<i>n</i> = 6 (S.D.)	<i>n</i> = 5 (S.D.)	
SiO <sub>2</sub>	58.75 (0.17)	57.55 (0.46)	55.71 (0.76)	54.99 (0.42)	
TiO <sub>2</sub>	1.85 (0.05)	0.96 (0.02)	1.20 (0.07)	1.69 (0.04)	
Al <sub>2</sub> O <sub>3</sub>	16.45 (0.14)	15.53 (0.17)	15.02 (0.28)	14.86 (0.16)	
FeO	0.98 (0.10)	1.66 (0.09)	1.42 (0.20)	1.38 (0.06)	
MgO	1.07 (0.02)	1.94 (0.25)	1.60 (0.69)	1.10 (0.11)	
CaO	0.81 (0.04)	1.61 (0.04)	1.51 (0.09)	1.51 (0.04)	
Na <sub>2</sub> O	5.97 (0.08)	5.66 (0.18)	5.37 (0.20)	5.30 (0.15)	
K <sub>2</sub> O	9.11 (0.07)	2.97 (0.07)	5.90 (0.31)	8.49 (0.12)	
Total	95.00 (0.53)	87.90 (0.40)	87.73 (1.98)	89.33 (0.84)	

In this and the following tables, *n* denotes number of analyses and bracketed figures are one standard deviation of the mean value.

<sup>a</sup> Alkali elements adjusted to allow for loss under near-focused electron microprobe beam (determined by comparing analyses from other runs where both defocused and near-focused beams were used).

(in apatite component proportions) were added for a Ti-saturated series and a P-saturated series. This gave a total of six compositions for experiments on the metaluminous series. These series essentially replicate an I-type metaluminous and calcalkaline granitic series, with variable  $K_2O/Na_2O$  from 0.26 to 3.1 (becoming increasingly alkaline as  $K_2O$  increases, but never peralkaline) (see Table 1).

The alkaline series were based on an interstitial glass composition from a peridotitic xenolith (DG-1 from Draper and Green, 1997), but to give a range of  $K_2O/Na_2O$  ratios, one member of each composition series was prepared with less  $K_2O$  than DG-1, and a third member of each composition series with more  $K_2O$  than DG-1.  $TiO_2$  and  $P_2O_5$  were added

for a Ti-saturated series and a P-saturated series. This gave a total of six compositions for experiments on the alkaline composition. The alkaline series approximate an A-type series, with variable  $K_2O/Na_2O$ . These alkaline series compositions vary from having an alumina saturation index (ASI) of 0.7–1.09. Only the lowest  $K_2O/Na_2O$  member of the P-enriched composition series is peraluminous (ASI=1.09). In addition, these series vary from alkaline for the low  $K_2O/Na_2O$  members through to clearly peralkaline for the highest  $K_2O/Na_2O$  members (see Table 1).

All compositions were prepared from analytical grade reagents (oxides or carbonates), ground together, fired, melted and then quenched to a glass. The glass

Table 3  
Analyses of glasses from the Ti-rich mineral saturated metaluminous T (TRN) series

Composition	TRNTiK	TRNTiKK	TRNTi	TRNTiK
Run number	R30	R30	R37	R31
Pressure (GPa)	0.5	0.5	1.5	1.5
Water (wt.%)	5	5	10	10
	<i>n</i> = 10 (S.D.)	<i>n</i> = 10 (S.D.)	<i>n</i> = 15 (S.D.)	<i>n</i> = 10 (S.D.)
SiO <sub>2</sub>	61.57 (0.56)	61.28 (0.24)	60.60 (0.33)	59.03 (0.67)
TiO <sub>2</sub>	2.45 (0.05)	2.11 (0.05)	1.07 (0.03)	1.22 (0.05)
Al <sub>2</sub> O <sub>3</sub>	15.95 (0.11)	16.43 (0.08)	15.26 (0.12)	15.44 (0.11)
FeO	2.28 (0.11)	1.56 (0.08)	2.58 (0.09)	1.97 (0.10)
MgO	0.80 (0.03)	0.56 (0.02)	0.98 (0.04)	0.77 (0.02)
CaO	2.83 (0.04)	1.97 (0.03)	3.63 (0.06)	2.77 (0.08)
Na <sub>2</sub> O	3.70 (0.09)	2.64 (0.06)	3.89 (0.09)	3.51 (0.06)
K <sub>2</sub> O	4.73 (0.04)	8.14 (0.10)	1.26 (0.02)	4.54 (0.09)
Total	94.34	94.71	89.27	89.27
Composition	TRNTiKK	TRNTi	TRNTiK	TRNTiKK
Run number	R31	1873	1873	1873
Pressure (GPa)	1.5	2.5	2.5	2.5
Water (wt.%)	10	10	10	10
	<i>n</i> = 10 (S.D.)	<i>n</i> = 12 (S.D.)	<i>n</i> = 8 (S.D.)	<i>n</i> = 12 (S.D.)
SiO <sub>2</sub>	58.40 (0.15)	62.77 (0.89)	62.06 (0.82)	62.05 (0.95)
TiO <sub>2</sub>	1.11 (0.03)	0.47 (0.08)	0.37 (0.05)	0.34 (0.06)
Al <sub>2</sub> O <sub>3</sub>	15.45 (0.08)	14.66 (0.26)	15.03 (0.21)	14.75 (0.23)
FeO	1.31 (0.07)	2.01 (0.13)	1.15 (0.04)	0.75 (0.07)
MgO	0.52 (0.02)	0.57 (0.05)	0.26 (0.01)	0.08 (0.02)
CaO	1.87 (0.05)	2.97 (0.11)	1.73 (0.05)	1.26 (0.09)
Na <sub>2</sub> O	2.33 (0.03)	4.14 (0.05)	3.6 <sup>a</sup>	2.9 <sup>a</sup>
K <sub>2</sub> O	7.75 (0.10)	1.41 (0.05)	4.7 <sup>a</sup>	7.1 <sup>a</sup>
Total	88.73	89.02	88.93	89.28

<sup>a</sup> Alkali elements adjusted to allow for loss under near-focused electron microprobe beam (determined by comparing analyses from other runs where both defocused and near-focused beams were used).

was then crushed, melted and quenched a second time, before final grinding to an average grain size of <20  $\mu\text{m}$  for the glass powder used in experiments. Several glass fragments from the final stage were kept for electron probe analysis to confirm each composition and to check homogeneity. Starting compositions are given in Table 1, as determined on these glass fragments.

## 2.2. High-pressure techniques

The experiments were conducted in a 1.27-cm piston-cylinder apparatus using standard techniques

(e.g. Green and Pearson, 1985). Talc-Pyrex sleeves were used as the pressure-transmitting medium and a  $-10\%$  correction was applied to nominal pressures (Green et al., 1966). Air-fired boron nitride and pyrophyllite spacers or sleeves were used within the graphite furnace. Five milligrams of sample were loaded into  $\text{Ag}_{70}\text{Pd}_{30}$  capsules, together with 5–10 wt.% water added with a microsyringe. Temperatures were measured with a Pt/Pt10%Rh thermocouple, for which no correction was made for any pressure effect on the emf. Temperatures were controlled to within  $\pm 2^\circ\text{C}$  of the set point and, allowing for temperature gradient within the triple capsule pressure cells, are

Table 4  
Analyses of glasses from the apatite saturated alkaline (DG) series

Composition	DG*P	DGP	DGPK	DG*P	DGP	DGPK
Run number	1856	1856	1856	1863	1901	1901
Pressure (GPa)	0.5	0.5	0.5	1.5	1.5	1.5
Water (wt.%)	5	5	5	5	5	5
	<i>n</i> = 10 (S.D.)	<i>n</i> = 10 (S.D.)	<i>n</i> = 10 (S.D.)	<i>n</i> = 10 (S.D.)	<i>n</i> = 10 (S.D.)	<i>n</i> = 11 (S.D.)
SiO <sub>2</sub>	59.95 (0.45)	58.13 (0.44)	57.92 (0.37)	60.27 (0.17)	59.49 (0.38)	58.06 (0.30)
TiO <sub>2</sub>	0.44 (0.03)	0.40 (0.02)	0.38 (0.02)	0.44 (0.05)	0.24 (0.02)	0.18 (0.03)
Al <sub>2</sub> O <sub>3</sub>	17.99 (0.11)	17.14 (0.14)	17.11 (0.07)	17.65 (0.13)	17.71 (0.08)	16.00 (0.16)
FeO	1.68 (0.05)	1.63 (0.07)	1.52 (0.08)	1.34 (0.09)	1.21 (0.09)	1.40 (0.07)
MgO	1.93 (0.04)	1.86 (0.04)	1.80 (0.03)	1.60 (0.22)	0.97 (0.05)	1.16 (0.04)
CaO	1.62 (0.05)	1.33 (0.03)	1.02 (0.04)	1.43 (0.05)	0.77 (0.03)	0.70 (0.04)
Na <sub>2</sub> O	6.19 (0.07)	5.46 (0.06)	5.73 (0.09)	6.33 (0.47)	6.34 (0.18)	6.02 (0.22)
K <sub>2</sub> O	4.26 (0.06)	7.12 (0.07)	9.67 (0.09)	4.38 (0.10)	7.33 (0.10)	8.81 (0.11)
P <sub>2</sub> O <sub>5</sub>	1.04 (0.05)	0.98 (0.03)	0.75 (0.05)	1.00 (0.05)	0.77 (0.07)	0.63 (0.07)
Total	95.10	94.07	95.91	94.51	94.88	93.03
Composition	DG*P	DGP	DGPK	DG*P	DGP	DGPK
Run number	1857	1857	1857	1899	1899	1899
Pressure (GPa)	2.5	2.5	2.5	3.5	3.5	3.5
Water (wt.%)	10	10	10	10	10	10
	<i>n</i> = 10 (S.D.)	<i>n</i> = 10 (S.D.)	<i>n</i> = 10 (S.D.)	<i>n</i> = 5 (S.D.)	<i>n</i> = 16 (S.D.)	<i>n</i> = 11 (S.D.)
SiO <sub>2</sub>	57.43 (0.28)	56.95 (0.26)	56.55 (0.45)	58.61 (1.02)	57.44 (1.11)	56.28 (0.54)
TiO <sub>2</sub>	0.41 (0.03)	0.26 (0.02)	0.22 (0.01)	0.43 (0.02)	0.20 (0.05)	0.14 (0.05)
Al <sub>2</sub> O <sub>3</sub>	17.11 (0.10)	15.76 (0.10)	15.96 (0.13)	14.64 (0.30)	14.87 (0.24)	15.05 (0.18)
FeO	1.53 (0.08)	1.60 (0.07)	1.35 (0.07)	0.75 (0.08)	0.68 (0.25)	0.40 (0.11)
MgO	1.60 (0.08)	1.67 (0.02)	1.03 (0.07)	1.27 (0.13)	0.67 (0.43)	0.20 (0.26)
CaO	1.70 (0.04)	1.46 (0.04)	0.81 (0.03)	0.71 (0.10)	0.45 (0.17)	0.20 (0.16)
Na <sub>2</sub> O	5.40 (0.08)	5.08 (0.08)	5.39 (0.11)	6.0 <sup>a</sup>	5.5 <sup>a</sup>	5.5 <sup>a</sup>
K <sub>2</sub> O	3.93 (0.10)	6.01 (0.04)	8.45 (0.10)	4.89 (0.45)	7.42 (0.39)	9.71 (0.50)
P <sub>2</sub> O <sub>5</sub>	1.14 (0.05)	1.13 (0.05)	0.79 (0.07)	2.14 (0.11)	2.11 (0.16)	1.90 (0.11)
Total	90.26	89.93	90.58	89.43 (0.74)	89.34 (1.06)	89.40 (0.74)

<sup>a</sup> Alkali elements adjusted to allow for loss under near-focused electron microprobe beam (determined by comparing analyses from other runs where both defocused and near-focused beams were used).

believed accurate to  $\pm 15$  °C. Conveniently, experiments were conducted with three capsules, each with a different K content, for each of the P- or Ti-saturated alkaline or T series. Occasionally, single capsule experiments (with 15 mg of sample) were carried out when it was necessary to repeat a run for a particular composition (e.g. if water loss occurred from one of the three capsules). All experiments were hydrous, with water contents varied to try to obtain near-isothermal near-liquidus conditions over the pressure range of 0.5–3.5 GPa. Experiments were conducted at 1000 °C for 24 h.

### 2.3. Analytical techniques

Electron microprobe analyses for major elements were obtained using a CAMECA® SX50 instrument at Macquarie University (see Adam and Green, 1994 for evaluation of accuracy and precision). Generally, a beam diameter of 30  $\mu\text{m}$  was used for analysis of glasses or quenched matrices, but this was reduced to 10  $\mu\text{m}$  in a few cases where glass areas were peppered with fine-grained crystals. An accelerating voltage of 15 kV and current of 20 nA were used, together with counting times of 10 s on peak and 5 s on each

Table 5  
Analyses of glasses from the apatite saturated metaluminous T (TRN) series

Composition	TRNPK	TRNP	TRNPK	TRNPKK	TRNP
Run number	R39	R40	R40R40		R58
Pressure (GPa)	0.5	1.5	1.5	1.5	2.5
Water (wt.%)	5	10	10	10	10
	<i>n</i> = 7 (S.D.)	<i>n</i> = 13 (S.D.)	<i>n</i> = 12 (S.D.)	<i>n</i> = 14 (S.D.)	<i>n</i> = 8 (S.D.)
SiO <sub>2</sub>	65.30 (0.48)	64.89 (0.53)	60.47 (0.33)	59.81 (0.21)	62.99 (0.39)
TiO <sub>2</sub>	0.23 (0.02)	0.30 (0.03)	0.22 (0.03)	0.16 (0.02)	0.31 (0.03)
Al <sub>2</sub> O <sub>3</sub>	16.10 (0.09)	16.19 (0.11)	15.37 (0.09)	15.69 (0.10)	15.59 (0.15)
FeO	2.18 (0.06)	2.81 (0.10)	2.02 (0.08)	1.38 (0.09)	2.51 (0.08)
MgO	0.82 (0.02)	1.02 (0.03)	0.73 (0.03)	0.50 (0.02)	0.90 (0.02)
CaO	3.02 (0.05)	4.41 (0.08)	3.31 (0.09)	2.33 (0.04)	4.13 (0.07)
Na <sub>2</sub> O	3.66 (0.04)	2.74 (0.08)	3.23 (0.06)	2.31 (0.05)	4.11 (0.18)
K <sub>2</sub> O	5.15 (0.07)	1.15 (0.03)	4.49 (0.06)	7.64 (0.08)	1.26 (0.03)
P <sub>2</sub> O <sub>5</sub>	0.34 (0.03)	0.47 (0.04)	0.45 (0.05)	0.32 (0.05)	0.49 (0.03)
Total	96.79 (0.47)	93.98 (0.50)	90.28 (0.31)	90.12 (0.29)	92.28 (0.51)
Composition	TRNPK	TRNPKK	TRNP	TRNPK	TRNPKK
Run number	R58	R58	R60	R60	R60
Pressure (GPa)	2.5	2.5	3.5	3.53.5	
Water (wt.%)	10	10	10	10	10
	<i>n</i> = 6 (S.D.)	<i>n</i> = 11 (S.D.)	<i>n</i> = 14 (S.D.)	<i>n</i> = 15 (S.D.)	<i>n</i> = 12 (S.D.)
SiO <sub>2</sub>	65.82 (1.05)	62.06 (0.28)	63.94 (0.25)	65.53 (0.69)	61.95 (0.21)
TiO <sub>2</sub>	0.21 (0.03)	0.17 (0.02)	0.27 (0.02)	0.21 (0.03)	0.14 (0.02)
Al <sub>2</sub> O <sub>3</sub>	16.48 (0.12)	16.19 (0.15)	15.22 (0.12)	15.30 (0.12)	16.20 (0.13)
FeO	1.53 (0.10)	1.46 (0.06)	1.71 (0.06)	1.04 (0.07)	0.85 (0.06)
MgO	0.42 (0.03)	0.54 (0.03)	0.52 (0.04)	0.22 (0.03)	0.28 (0.02)
CaO	2.78 (0.07)	2.36 (0.08)	3.41 (0.09)	1.98 (0.09)	1.78 (0.04)
Na <sub>2</sub> O	2.75 (0.81)	2.43 (0.07)	3.58 (0.15)	2.94 (0.57)	2.69 (0.08)
K <sub>2</sub> O	4.77 (0.08)	7.81 (0.07)	1.37 (0.04)	5.32 (0.15)	8.31 (0.11)
P <sub>2</sub> O <sub>5</sub>	0.34 (0.02)	0.33 (0.04)	0.41 (0.03)	0.27 (0.04)	0.24 (0.02)
Total	95.10 (0.73)	93.34 (0.42)	90.42 (0.25)	92.83 (0.68)	92.43 (0.31)

background. Correction procedures followed the PAP routine (Pouchou and Pichoir, 1984).

### 3. Results

Average analyses for glasses saturated in a P-rich mineral (apatite) or a Ti-rich mineral (rutile; earlier work showed that TiO<sub>2</sub> content at Ti-mineral saturation was not affected by the nature of the Ti-rich mineral; Green and Pearson, 1986) are presented in Tables 2–5. Because this study is directed at compositional effects other than SiO<sub>2</sub> content variation, the analyses from Tables 2–5 have been corrected to a constant SiO<sub>2</sub> content of 65 wt.%, first by recalculating to 100% to remove the variable water content which at these high levels essentially behaves as a dilutant. Then, the TiO<sub>2</sub>

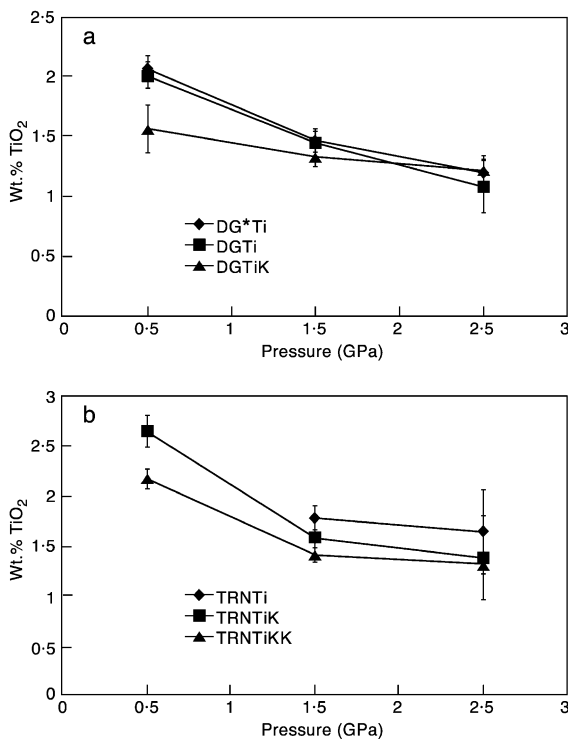


Fig. 1. TiO<sub>2</sub> content of glass at Ti-rich mineral saturation as a function of pressure. In this and the following figures, analyses have been adjusted to an anhydrous total and fixed SiO<sub>2</sub> content of 65 wt.% (see text). In addition, abbreviations for compositions are same as given in Table 1. (a) Alkaline composition series. (b) Metaluminous T composition series.

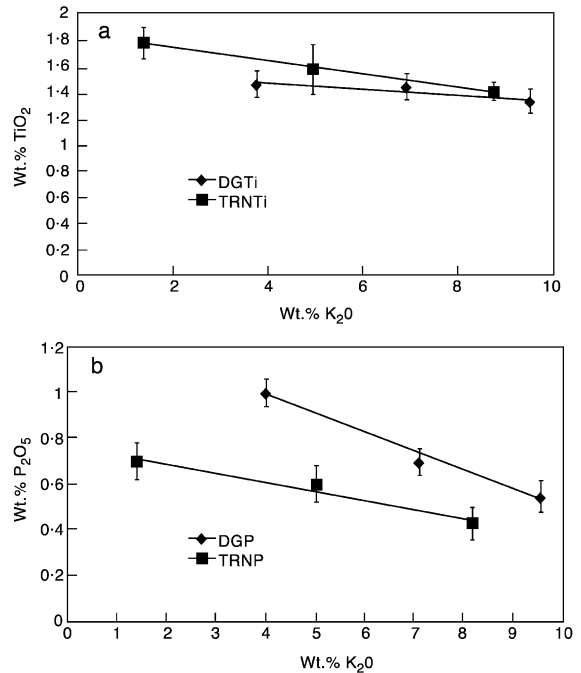


Fig. 2. (a) TiO<sub>2</sub> content of glass at Ti-mineral saturation or (b) P<sub>2</sub>O<sub>5</sub> content of glass at apatite saturation as a function of K<sub>2</sub>O content at a fixed pressure of 1.5 GPa.

or P<sub>2</sub>O<sub>5</sub> contents have been adjusted to new values consistent with SiO<sub>2</sub> of 65 wt.% using established TiO<sub>2</sub> or P<sub>2</sub>O<sub>5</sub> variation with SiO<sub>2</sub> from this work and from earlier studies (e.g. Ryerson and Watson, 1987 for TiO<sub>2</sub> contents and from Green and Watson, 1982 for P<sub>2</sub>O<sub>5</sub> contents). The adjustment values used were 0.2% TiO<sub>2</sub> and 0.05% P<sub>2</sub>O<sub>5</sub> change for each 1% SiO<sub>2</sub> change from 65 wt.%. These recalculated TiO<sub>2</sub> or P<sub>2</sub>O<sub>5</sub> contents are then presented in Figs. 1–3, which now allow evaluation of TiO<sub>2</sub> or P<sub>2</sub>O<sub>5</sub> contents at rutile or apatite saturation as a function only of pressure and/or K<sub>2</sub>O content variation.

#### 3.1. Ti saturation

Fig. 1 shows that the TiO<sub>2</sub> content at Ti-mineral saturation decreases with increasing pressure for both the alkaline and T series. The latter series shows a relatively sharp decrease in Ti-mineral solubility between 0.5 and 1.5 GPa, followed by a slight decrease between 1.5 and 2.5 GPa, contrasting with the alkaline series that shows a relatively uniform

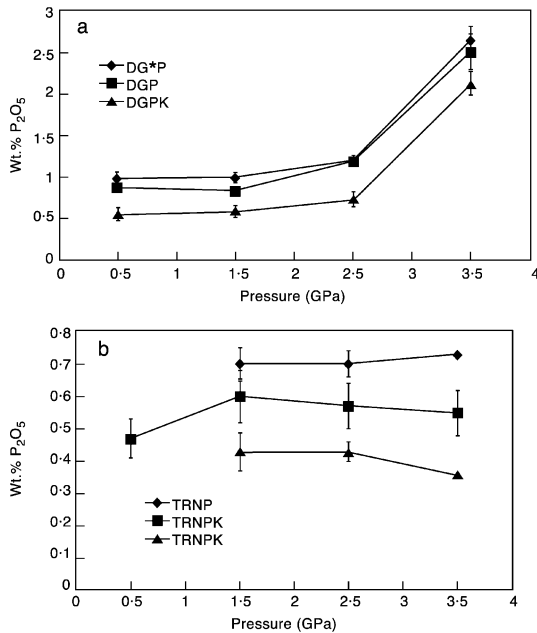


Fig. 3. P<sub>2</sub>O<sub>5</sub> content of glass at apatite saturation as a function of pressure. (a) Alkaline composition series. (b) Metaluminous T composition series.

decrease in solubility over the 0.5–2.5 GPa range. The net result of this behaviour is that the Ti-mineral solubility is lower in the alkaline series compared with the T series at 0.5 GPa, but is similar at 1.5–2.5 GPa. Fig. 2a plots TiO<sub>2</sub> content at Ti-mineral saturation as a function of K<sub>2</sub>O content at a fixed pressure of 1.5 GPa. This shows that increasing melt K<sub>2</sub>O content reduces Ti-mineral solubility for the T series, but has no effect (within error) for the alkaline series.

### 3.2. P saturation

Fig. 3 shows that the P<sub>2</sub>O<sub>5</sub> content at P-mineral saturation increases with decreasing K<sub>2</sub>O content (or decreasing K<sub>2</sub>O/Na<sub>2</sub>O ratio) of the melt for both the alkaline and T series. However, pressure has no effect on P-mineral solubility, apart from the 3.5 GPa experiment on the alkaline composition that shows a sharp increase in solubility. Overall, the solubility of P-minerals is higher in the alkaline compared with T series compositions. The relationship between P-mineral saturation and K<sub>2</sub>O content for both series is shown in Fig. 2b, with a steady decrease in P-mineral

solubility with increasing K<sub>2</sub>O content (at a fixed pressure of 1.5 GPa).

## 4. Discussion of results

### 4.1. Silicate liquid structure

In terms of structural models for silicate liquids, based on nonbridging oxygens per tetrahedral cation (NBO/T) (e.g. Mysen, 1990), the solubility of both Ti-rich and P-rich minerals is expected to decrease as melts become more SiO<sub>2</sub>-rich and thus more polymerized (i.e. decrease in NBO/T) (Watson, 1979; Green and Watson, 1982; Green and Pearson, 1986; Ryerson and Watson, 1987; Watson and Capobianco, 1981). Furthermore, the essentially second order changes in solubility as a function of pressure and K<sub>2</sub>O content depicted in Figs. 1–3 can be assessed with reference to predictions based on models of silicate liquid structure. Because all melts in this study are SiO<sub>2</sub>-rich, broadly granitic and relatively polymerized, this evaluation focuses on effects at the low NBO/T end of the natural silicate liquid spectrum.

#### 4.1.1. Ti-mineral saturation

The decrease in Ti-mineral solubility with increasing pressure could most simply imply that polymerization increases as pressure increases. However, the effect of pressure on silicate liquid structure is complex, especially in relation to the role of Ti in the structure. Although Ti in glasses and melts is known to exist in coordination states ranging from three to six (e.g. Farges et al., 1996; Farges, 1997; Farges and Brown, 1997), its preferred coordination state is six (as occurs in rutile). Paris et al. (1994) showed that increased pressure promoted increase in coordination of Ti (i.e. to sixfold coordination). This should favour crystallization of Ti-rich minerals (with Ti in sixfold coordination) and, consequently, a decrease in Ti-rich mineral solubility. This is consistent with the behaviour shown in Fig. 1a. Thus, the changes in TiO<sub>2</sub> solubility accompanying changes in pressure (see Figs. 1a and 3a) may be understood in terms of the influence that these factors have on the ability of Ti to achieve its favoured sixfold coordination state. For example, weakening of the Si–O bond as a result of increasing pressure (Bottinga and Richet, 1995) may



enable Ti to more effectively compete for oxygens within the Si–O–Ti network. Similarly, both the breaking of Si–O bonds caused by the addition of K and the substitution of weaker Al–O bonds (in  $\text{KAlO}_4$ ) may also enable Ti to compete more effectively for oxygens, thus promoting Ti-mineral saturation.

The impact of K, or increased  $\text{K}_2\text{O}/\text{Na}_2\text{O}$  ratio, on the behaviour of silicate liquid is expected to be greater than other potential network modifiers because of K's higher mean molar volume relative to change in concentration (Bottinga and Richet, 1995). Thus, it is expected that  $\text{K}_2\text{O}$  content would have an effect on both Ti-mineral and P-mineral solubilities. K may be linked via charge balancing with Al or  $\text{Fe}^{3+}$  in a network-forming arrangement, with increasing K causing an increase in polymerization and a decrease in solubility, as observed for the T series. However, this is not the anticipated behaviour for peralkaline compositions (such as the most K-rich compositions in the alkaline series) where increased K acts as a network modifier, decreasing polymerization and hence resulting in an expected increase in Ti-mineral solubility. Gwinn and Hess (1989) used simple systems to predict just this type of behaviour, as they argued that excess K (as in peralkaline melts) should stabilize Ti in fourfold coordination in melts and so increase Ti-mineral solubility. In the natural system, at 0.5–2.5 GPa, we observed no effect of increased  $\text{K}_2\text{O}$  content on Ti-mineral solubility in the alkaline composition series, at least within error. Nor was there an increased solubility in the alkaline compared with the T series at 0.5–2.5 GPa, suggesting that the impact of high pressure favouring higher coordination states for Ti outweighs the effect of added  $\text{K}_2\text{O}$  on Ti coordination.

#### 4.1.2. P-mineral saturation

In parallel with the discussion for Ti, the results in Figs. 2b and 3 imply that decreasing solubility of P with increasing  $\text{K}_2\text{O}$  means that the silicate liquid structure becomes more polymerized with increasing  $\text{K}_2\text{O}$  content. However, in contrast to Ti, P solubility appears unaffected by pressure, except at 3.5 GPa for the alkaline composition where solubility shows a marked increase. This lack of effect of pressure may be due to there being no change in coordination state of P in silicate liquids as pressure changes (in contrast

to Ti). The result at 3.5 GPa is striking and points to depolymerization in these compositions at this pressure, irrespective of  $\text{K}_2\text{O}$  content. The role of P in silicate liquid structures is multiconfigurational, i.e. P readily co-polymerizes with Si in tetrahedral coordination with oxygen (unlike Ti) (Ryerson and Hess, 1980; Mysen et al., 1981) and links with network-modifying alkali cations or aluminium to form complexes (Toplis and Dingwell, 1996). Thus, P complexes are stabilized in more alkaline relative to less alkaline melts (suppressing P-mineral saturation). This is consistent with the higher P-mineral solubility observed in the alkaline series compared with the T series. However, it does not explain the decreasing P-mineral solubility with increasing  $\text{K}_2\text{O}$  content in both compositions. Following the same argument, an increase in P-mineral solubility would have been expected. Such an anomaly points to greater complexities in the natural system, with regard to interrelationships of P and alkali elements, than predicted from the simple system work. A final point that needs to be acknowledged for P-mineral solubility is that saturation may equally depend on the activity of other components (e.g. Ca in the case of apatite) (Bea et al., 1992; Toplis and Dingwell, 1996). This is particularly relevant for the alkaline series, where the two K-rich compositions had slightly less CaO than required by the  $\text{P}_2\text{O}_5$  present to form apatite. In contrast, each of the metaluminous T series compositions had “excess” CaO over  $\text{P}_2\text{O}_5$ . Despite this caveat, the patterns of P-mineral solubility appear consistent irrespective of CaO content in the compositions examined.

#### 4.2. Application to granitic magmas

For all A- and I-type granitic suites, potential P-mineral (typically apatite) fractionation and potential Ti-mineral (typically titanite, ilmenite or rutile) fractionation are likely for evolved members of these suites. This will result in depletion of derivative magmas in middle rare earth elements (REE) (because apatite and titanite favour these elements; Green, 1994) and in high field strength elements (HFSE) (because titanite, ilmenite and rutile readily accommodate these; Green, 1994). In general, I-type suites will show lower solubility for P-minerals compared with A-type suites and hence greater potential for

fractionation of these minerals in evolved members of the suite. The solubility of Ti-minerals does not appear to be significantly different for evolved A- or I-type suites; however, potential Ti-mineral fractionation in A-type suites may be complicated by crystallization of Ti-bearing alkaline ferromagnesian minerals, and P-mineral fractionation may involve monazite as well as apatite. For I-type suites with different  $K_2O/Na_2O$  ratios, potential fractionation of P-minerals will be greater for the suites with highest  $K_2O/Na_2O$ . This will mean that these minerals could crystallize at an earlier stage of magmatic evolution in the high  $K_2O/Na_2O$  suites, with consequent effects on the REE distribution in the more evolved magmas from these suites. A further aspect that applies in extremely evolved granitic compositions, where concentrations of REE and HFSE may reach “minor element” levels, is the possible effect these elements may have on Ti- or P-mineral solubility. Exploratory experiments at 2.5 GPa and 1000 °C directed at this point showed that addition of HFSE to both compositions either had no effect (within error) or else increased the solubility of the Ti-mineral slightly (12–20%). Addition of REE clearly reduced the solubility of apatite in both compositions by 35–40% (see also Wolf and London, 1995).

The results also have application to the process of magma mingling that Vernon (1983) highlighted as important in the generation of enclave-bearing granitic suites. Any enclave selvage that reflects interaction between mingling mafic and felsic magmas would be expected to show crystallization of apatite from the mafic magma because of imposition on the mafic magma of lower T, higher  $SiO_2$  (factors already well established as reducing P solubility, e.g. Watson, 1979; Green and Watson, 1982; Watson and Capobianco, 1981) and higher  $K_2O/Na_2O$  (shown in this study to reduce P solubility) through contact with the felsic magma. An equivalent effect for Ti-mineral saturation would also be expected, but may occur less readily because of relatively higher contents of  $TiO_2$  needed for saturation and because of take-up of  $TiO_2$  in crystallizing mafic minerals.

#### 4.3. Application to subduction zones

Earlier work (e.g. Foley and Wheller, 1990) has pointed out that a low-degree hydrous trondhjemitic

melt from the subducted oceanic crust is likely to be saturated in a Ti-mineral at its source at depth, but the present results now show that the same magma at shallower levels will not be saturated because of the increasing solubility of  $TiO_2$  with decreasing pressure. Thus, any residual Ti-mineral carried up from subducted oceanic crust source region will subsequently dissolve as the magma rises to shallower levels. This contrasts with apatite, which is likely to be a fractionating mineral from source to level of emplacement or surface, because of its unchanged solubility with decreasing pressure. For the complete spectrum of magmas in subduction zones that includes high-K magmas with  $K_2O/Na_2O > 1$  (e.g. Gill, 1981), saturation in apatite will be achieved at an earlier stage of fractionation in the high-K magma series. In addition, the results concerning the pressure effect on Ti-mineral solubility have application to the type of model proposed by Sajona et al. (1996) to explain the origin of Nb- (and Ti) rich basalts and basaltic andesites associated with adakites in some subduction zones. They envisaged initial slab melts (adakites) rising into and metasomatizing the peridotitic mantle wedge at relatively low pressure where Ti has greater solubility. This metasomatized wedge peridotite is then dragged to deeper levels as subduction proceeds, and undergoes melting to produce the Nb- (and Ti) rich more mafic magmas. Although at these deeper levels the solubility of  $TiO_2$  is less, this effect is more than counteracted by the increased solubility in the more silica poor mafic magmas generated at this stage compared with adakites. Thus, this is consistent with higher Ti (and Nb) in mafic melts derived at this stage from the metasomatized mantle wedge.

#### 4.4. Application to mantle metasomatism

As noted in Introduction, the alkaline composition was modelled on an interstitial glass from a peridotitic xenolith. This type of glass had been considered as a possible metasomatizing melt in the upper mantle (e.g. Zinngrebe and Foley, 1995; Wulff-Pedersen et al., 1996, 1999; Draper and Green, 1997). The present results provide constraints on the potential P-mineral and Ti-mineral “carrying capacity” of such a melt, as it moves to shallower levels in the mantle where P-mineral crystallization will be unchanged, but Ti-mineral crystallization will be inhibited. The new

results also point to different “carrying capacities” for melts with differing  $K_2O/Na_2O$  ratios, decreasing with increasing  $K_2O/Na_2O$  ratio.

## 5. Conclusions

Evolving granitic magmas will eventually become saturated in both Ti- and P-rich minerals, but the stage (most simply viewed as the  $SiO_2$  content) at which this occurs in the fractionation process will vary, depending on temperature (linked most closely to water content), pressure, alkali element content and  $K_2O/Na_2O$  ratio. The link of decreasing solubility with decreasing temperature (usually accompanying increasing water content) is well established (e.g. Watson, 1979; Green and Watson, 1982; Green and Pearson, 1986; Ryerson and Watson, 1987; Watson and Capobianco, 1981), but the present study on granitic compositions has also shown that the solubility of the P-mineral group decreases with increasing alkali element content and increasing  $K_2O/Na_2O$  ratio. The pressure effect differs for the two mineral groups, with the Ti-mineral group showing an increase in solubility with decreasing pressure, but the P-mineral group generally showing no change in solubility with decreasing pressure (with the exception of the alkaline compositions at 3.5 GPa). The different results for the alkaline series (cf. A-type granites) and the metaluminous T series (cf. I-type granites) indicate that trace element distributions in I-type high-K granitic fractionates will potentially show the greatest effect of P- and Ti-mineral fractionation. This would characteristically appear as relative depletion in the middle REE (e.g. from apatite and titanite fractionation) and in the HFSE (e.g. from titanite or rutile fractionation).

## Acknowledgements

The friendship and support of Professor Ron Vernon over a very long time as a colleague at Macquarie University in teaching and research have been an abiding influence on us, and are most warmly acknowledged. This work has been supported by an ARC Small Grant to T.H.G. The hospitality of Dr. D. Ellis and the staff of the Geology Department, A.N.U., where this contribution has been written, is acknowl-

edged with thanks. Dr. C. Miller and Dr. M. Wolf constructively reviewed the manuscript and their suggested changes are gratefully recognized. This is publication number 239 from the Australian Research Council National Key Centre for the Geochemical Evolution and Metallogeny of Continents (GEMOC).

## References

- Adam, J., Green, T.H., 1994. The effects of pressure and temperature on the partitioning of Ti, Sr and REE between amphibole, clinopyroxene and basaltic melts. *Chem. Geol.* 117, 219–233.
- Bea, F., 1996. Residence of REE, Y, Th and U in granites and crustal protoliths; implications for the chemistry of crustal melts. *J. Petrol.* 37, 521–552.
- Bea, F., Fershtater, G., Corretge, L.G., 1992. The geochemistry of phosphorus in granitic rocks and the effect of aluminium. *Lithos* 29, 43–56.
- Bottinga, Y., Richet, P., 1995. Silicate melts: the “anomalous” pressure dependence of viscosity. *Geochim. Cosmochim. Acta* 59, 2725–2731.
- Bryant, C.M., Arculus, R.J., Chappell, B.W., 1997. The Clarence River supersuite: a 250 Ma Cordilleran tonalite analogue in eastern Australia. *J. Petrol.* 38, 975–1001.
- Champion, D.C., Chappell, B.W., 1992. Petrogenesis of felsic I-type granites: an example from northern Queensland. *Trans. R. Soc. Edinburgh: Earth Sci.* 83, 115–126.
- Chappell, B.W., 1999. Aluminium saturation in I- and S-type granites and the characterization of fractionated haplogranites. *Lithos* 46, 535–551.
- Draper, D.S., Green, T.H., 1997. P–T phase relationships of silicic, alkaline, aluminous mantle–xenolith glasses under anhydrous and C–O–H fluid-saturated conditions. *J. Petrol.* 38, 1187–1294.
- Drummond, M.S., Defant, M.J., 1990. A model for trondhjemite–tonalite–dacite genesis and crustal growth via slab melting: Archean to modern comparisons. *J. Geophys. Res.* 95, 503–521.
- Farges, F., 1997. Coordination of  $Ti^{4+}$  in silicate glasses: a high-resolution XANES study at the Ti K edge. *Am. Mineral.* 82, 36–43.
- Farges, F., Brown Jr., G.E., 1997. Coordination chemistry of Ti(IV) in silicate glasses and melts: IV. XANES studies of synthetic and natural volcanic glasses and tektites at ambient temperature and pressure. *Geochim. Cosmochim. Acta* 61, 1863–1870.
- Farges, F., Brown Jr., G.E., Navrotsky, A., Gan, H., Rehr, J.R., 1996. Coordination chemistry of Ti(IV) in silicate glasses and melts: III. Glasses and melts from ambient to high temperatures. *Geochim. Cosmochim. Acta* 60, 3055–3065.
- Foley, S., Wheller, G., 1990. Parallels in the origin of the geochemical signatures of island arc volcanics and continental potassic igneous rocks: the role of residual titanites. *Chem. Geol.* 85, 1–18.
- Gill, J.B., 1981. *Orogenic Andesites and Plate Tectonics* Springer-Verlag, Berlin, 399 pp.

- Green, T.H., 1981. Experimental evidence for the role of accessory phases in magma genesis. *J. Volcanol. Geotherm. Res.* 10, 405–422.
- Green, T.H., 1982. Anatexis of mafic crust and high pressure crystallization of andesite. In: Thorpe, R.S. (Ed.), *Andesites*, Wiley, New York, pp. 465–487.
- Green, T.H., 1994. Experimental studies of trace element partitioning applicable to igneous petrogenesis—Sedona 16 years later. *Chem. Geol.* 117, 1–36.
- Green, T.H., Pearson, N.J., 1985. Rare earth element partitioning between clinopyroxene and silicate liquid at moderate to high pressure. *Contrib. Mineral. Petrol.* 91, 24–36.
- Green, T.H., Pearson, N.J., 1986. Ti-rich phase saturation in hydrous mafic–felsic compositions at high P, T. *Chem. Geol.* 54, 185–201.
- Green, T.H., Watson, E.B., 1982. Crystallization of apatite in natural magmas under high pressure, hydrous conditions, with particular reference to ‘orogenic’ rock series. *Contrib. Mineral. Petrol.* 79, 96–105.
- Green, T.H., Ringwood, A.E., Major, A., 1966. Friction effects and pressure calibration in a piston-cylinder apparatus at high pressure and temperature. *J. Geophys. Res.* 71, 3589–3594.
- Gromet, L.P., Silver, L.T., 1983. Rare earth element distribution among minerals in a granodiorite and their petrogenetic implications. *Geochim. Cosmochim. Acta* 47, 925–940.
- Gwinn, R., Hess, P.C., 1989. Iron and titanium solution properties in peraluminous and peralkaline rhyolitic liquids. *Contrib. Mineral. Petrol.* 101, 326–338.
- King, P.L., White, A.J.R., Chappell, B.W., Allen, C.M., 1997. Characterization and origin of aluminous A-type granites from the Lachlan Fold Belt, southeastern Australia. *J. Petrol.* 38, 371–391.
- Miller, C.F., Mittlefehdt, D.W., 1982. Light rare earth element depletion in felsic magmas. *Geology* 10, 129–133.
- Mysen, B.O., 1990. Relationships between silicate melt structure and petrologic processes. *Earth-Sci. Rev.* 27, 281–365.
- Mysen, B.O., 1998. Phosphorus solubility mechanisms in haplogranitic aluminosilicate glass and melt: effect of temperature and aluminium content. *Contrib. Mineral. Petrol.* 133, 38–50.
- Mysen, B.O., Ryerson, F.J., Virgo, D., 1981. The structural role of phosphorus in silicate melts. *Am. Mineral.* 66, 106–117.
- Paris, E., Dingwell, D.B., Seifert, F.A., Mottana, A., Romano, C., 1994. Pressure-induced coordination change of Ti in silicate glass: a XANES study. *Phys. Chem. Miner.* 21, 510–515.
- Pouchou, J.L., Pichoir, F., 1984. A new model for quantitative X-ray microanalysis: Part I. Applications to the analysis of homogeneous samples. *Rech. Aerosp.* 3, 13–38.
- Ryerson, F.J., Hess, P.C., 1980. The role of P<sub>2</sub>O<sub>5</sub> in silicate melts. *Geochim. Cosmochim. Acta* 44, 611–624.
- Ryerson, F.J., Watson, E.B., 1987. Rutile saturation in magmas: implications for Ti–Nb–Ta depletion in island arc basalts. *Earth Planet. Sci. Lett.* 86, 225–239.
- Sajona, F.G., Maury, R.C., Bellon, H., Cotton, J., Defant, M., 1996. High field strength element enrichment of Pliocene–Pleistocene island arc basalts, Zamboanga Peninsula, Western Mindanao (Philippines). *J. Petrol.* 37, 693–726.
- Sawka, W.N., 1988. REE and trace element variations in accessory minerals and hornblende from the strongly zoned McMurray Meadows Pluton, California, U.S.A. *Trans. R. Soc. Edinburgh: Earth Sci.* 79, 157–168.
- Sha, L.-K., 1998. Order–disorder kinetics in crystals, and phosphorus geochemistry of granites, with implications for lunar rocks and meteorites. Unpubl. PhD thesis, Aust. Nat. Univ., 329 pp.
- Toplis, M.J., Dingwell, D.B., 1996. The variable influence of P<sub>2</sub>O<sub>5</sub> on the viscosity of melts of differing alkali/aluminium ratio: implications for the structural role of phosphorus in silicate melts. *Geochim. Cosmochim. Acta* 60, 4107–4121.
- Vernon, R.H., 1983. Restite, xenoliths and microgranitoid xenoliths. *J. Proc. R. Soc. N. S. W.* 116, 77–103.
- Watson, E.B., 1979. Apatite saturation in basic to intermediate magmas. *Geophys. Res. Lett.* 6, 937–940.
- Watson, E.B., Capobianco, C.J., 1981. Phosphorus and the rare earth elements in felsic magmas: an assessment of the role of apatite. *Geochim. Cosmochim. Acta* 45, 2349–2358.
- Watson, E.B., Harrison, T.M., 1984. Accessory minerals and the geochemical evolution of crustal magmatic systems: a summary and prospectus of experimental approaches. *Phys. Earth Planet. Inter.* 35, 19–30.
- Watt, G.R., Harley, S.L., 1993. Accessory phase controls on the geochemistry of crustal melts and restites produced during water-undersaturated partial melting. *Contrib. Mineral. Petrol.* 114, 550–556.
- Wolf, M.B., London, D., 1994. Apatite dissolution into peraluminous haplogranitic melts: an experimental study of solubilities and mechanisms. *Geochim. Cosmochim. Acta* 58, 4127–4146.
- Wolf, M.B., London, D., 1995. Incongruent dissolution of REE- and Sr-rich apatite in peraluminous granitic liquids: differential apatite, monazite, and xenotime solubilities during anatexis. *Am. Mineral.* 80, 765–775.
- Wulff-Pedersen, E., Neumann, E.-R., Jensen, B.B., 1996. The upper mantle under La Palma, Canary Islands: formation of Si–K–Na-rich melt and its importance as a metasomatic agent. *Contrib. Mineral. Petrol.* 125, 113–139.
- Wulff-Pedersen, E., Neumann, E.-R., Vannucci, R., Botazzi, P., Ottolini, L., 1999. Silicic melts produced by reaction between peridotite and infiltrating basaltic melts: ion probe data on glasses and minerals in veined xenoliths from La Palma, Canary Islands. *Contrib. Mineral. Petrol.* 114, 550–556.
- Zinggribe, E., Foley, S.F., 1995. Metasomatism in mantle xenoliths from Gees, West Eifel, Germany: evidence for the genesis of calc-alkaline glasses and metasomatic Ca-enrichment. *Contrib. Mineral. Petrol.* 122, 79–96.